

Unified unquenched quark model for heavy-light mesons with chiral dynamics

Ru-Hui Ni¹, Jia-Jun Wu^{2,3} *, and Xian-Hui Zhong^{1,4} †

¹*Department of Physics, Hunan Normal University, and Key Laboratory of Low-Dimensional Quantum Structures and Quantum Control of Ministry of Education, Changsha 410081, China*

²*School of Physical Sciences, University of Chinese Academy of Sciences (UCAS), Beijing 100049, China*

³*Southern Center for Nuclear-Science Theory (SCNT), Institute of Modern Physics, Chinese Academy of Sciences, Huizhou 516000, Guangdong Province, China and*

⁴*Synergetic Innovation Center for Quantum Effects and Applications (SICQEA), Hunan Normal University, Changsha 410081, China*

In this work, an unquenched quark model is proposed for describing the heavy-light mesons by taking into account the coupled-channel effects induced by chiral dynamics. After including a relativistic correction term for the strong transition amplitudes, both the mass spectra and decay widths of the observed heavy-light mesons can be successfully described simultaneously in a unified framework, several long-standing puzzles related to the small masses and broad widths are overcome naturally. We also provide valuable guidance in searching new heavy-light mesons by the detailed predictions of their masses, widths, and branching ratios. The success of the unquenched quark model presented in this work indicates it may be an important step for understanding the hadron spectrum.

I. INTRODUCTION

The fundamental theory of strong interaction is Quantum Chromodynamics (QCD). One of its most prominent challenges is the phenomenon of confinement, the elementary systems we observe, known as hadrons and composed of quarks and gluons, appear to be colorless. In the low-energy regime, the non-perturbative effects make it impossible to achieve analytical computations. Lattice QCD simulation can provide the hadronic spectra from first principles, but it falls short of offering a detailed picture of hadrons. In such circumstances, a theoretical model becomes essential for gaining a deeper insight into the nature of confinement.

The quenched quark model, initially based solely on $q\bar{q}$ for mesons and qqq for baryons and developed in the 1960s by Gell-Mann and Zweig [1–3], effectively described the hadron spectrum until the discovery of the $X(3872)$ [4] and $D_s(2317)$ in 2003 [5]. Over the past two decades, an increasing number of hadron states, often referred to as ‘exotic’, have been observed [6]. These discoveries, including the XYZ and P_c states, have challenged the predictions of the simple $q\bar{q}$ and qqq models [7–35], more works in the reviews [36–38]. An undeniable factor contributing to this discrepancy is the omission of coupled-channel effects resulting from hadron loops in these quark models. This deficiency has long been recognized and discussed, for instance, in 1980, a similar effect known as the meson cloud was proposed [39]. This underscores the importance of considering interactions at both the quark(gluon) level and the hadron level to obtain a comprehensive understanding of physical hadrons.

The significance of coupled-channel effects is widely acknowledged within the scientific community. However, conducting a systematic study in practical calculations presents several challenging issues. The primary concerns can be summarized as follows:

- P1.** How to select the coupled-channels.
- P2.** How to obtain correct both mass and width.
- P3.** How to evaluate the coupled channel effects in the high momentum region.

All of these challenges add complexity when employing a comprehensive model. Consequently, existing research has primarily focused on exploring coupled-channel effects for states that deviate significantly from conventional quark models, rather than those with well-established explanations within the hadron spectrum. For instance, while considering loop contributions for scalar mesons, such as $K\bar{K}$ and $\pi\pi$ loops, only quark level interactions are accounted for ρ meson where the $\pi\pi$ loop indeed significantly shifts the mass of ρ . This lack of consistency and self-consistency within the theory arises as an issue. Furthermore, in the context of strong decay, systematic studies have been conducted within several phenomenological models [20–35], as detailed in recent reviews [37, 38]. However, these models often struggle to accurately describe the widths of higher resonances [37, 38].

In the past twenty years, numerous excited heavy-light meson candidates have been observed by collaborations such as D0, CDF, BABAR, and LHCb [6]. Most theoretical studies have primarily focused on near-threshold states, such as $D_{s0}^*(2317)$ and $D_{s1}(2460)$ [40–45], or have been limited to the D_s spectrum or D spectrum separately [46–48]. In comparison to the mass spectrum, $D_0(2550)/D_{s0}(2590)$ and $D_1^*(2600)/D_{s1}^*(2700)$ can be categorized as radial excitations. However, the predicted decay widths within the chiral quark model [30–35] systematically underestimate the observed values. Thus, a comprehensive investigation of both the mass spectra and decay widths for all heavy-light mesons, including D , D_s , B , and B_s mesons, within a unified framework that incorporates unquenched coupled-channel effects is currently lacking. This is a crucial step in the development of a comprehensive model for hadron physics.

In this work, we will fill this gap by introducing a unified unquenched quark model framework that accounts for coupled-channel effects, utilizing a semi-relativistic potential

*E-mail: wujiajun@ucas.ac.cn

†E-mail: zhongxh@hunnu.edu.cn

to interpolate both the masses and widths of all heavy-light mesons for the first time.

II. FRAMEWORK

In this model, as described in previous works [49–53], the Hamiltonian of the hadronic system is described by

$$\mathcal{H} = \mathcal{H}_0 + \mathcal{H}_c + \mathcal{H}_I. \quad (1)$$

Here, \mathcal{H}_0 represents the Hamiltonian governing the bare $Q\bar{q}$ state denoted as $|A\rangle$, and it is derived from the semi-relativistic quark potential model. \mathcal{H}_c is the noninteracting Hamiltonian for the continuum state $|BC\rangle$, while \mathcal{H}_I is an effective Hamiltonian for describing the coupling between $|A\rangle$ and $|BC\rangle$. The quark (gluon) level interactions are all encompassed within \mathcal{H}_0 , which are clearly defined, as introduced in the Supplemental Material [54]. Meanwhile, \mathcal{H}_I contains the hadronic interactions, which will be explored in detail.

To address the question posed in **P1** on the first page, the mass of a dressed hadron is estimated with the once-subtracted method suggested in Ref. [55], i.e.,

$$M = M_A - \text{Re} \sum_{BC} \int_0^\infty \frac{(M_0 - M) |\langle BC, \mathbf{q} | \mathcal{H}_I | A \rangle|^2}{(M - E_{BC})(M_0 - E_{BC})} q^2 dq, \quad (2)$$

where $\mathbf{q} \equiv (0, 0, q)$, and M_A is the bare mass determined by the \mathcal{H}_0 . M_0 represents the subtracted zero point for the heavy-light meson system. E_{BC} is the kinematic energy of the $|BC, \mathbf{q}\rangle$ continuum state with the loop momentum \mathbf{q} . We select the masses of the ground heavy-light meson states, namely $D_{(s)}$ and $B_{(s)}$, as the reference values denoted by M_0 . With the once-subtracted method, in the calculations one only need consider the OZI-allowed two-body hadronic channels with mass thresholds below or just above the bare $|A\rangle$ states. The contributions from the other virtual channels (whose mass thresholds far above the bare $|A\rangle$ states) are subtracted from the dispersion relation by redefining the bare mass. This method has been applied to study the coupled-channel effects on D/D_s meson states and charmonium states in the literature [46, 56]. It should be emphasized that the application of once-subtracted method is a crucial step for obtaining a successful description of the heavy-light meson spectrum within a unified unquenched quark model.

For a strong decay process $A \rightarrow BC$, the partial decay width is obtained by

$$\Gamma = 2\pi \frac{|\mathbf{q}| E_B E_C}{M} \overline{|\langle BC, \mathbf{q} | \mathcal{H}_I | A \rangle|^2}, \quad (3)$$

where \mathbf{q} and $E_{B/C}$ are the on-shell momentum and energy of particle B/C in the decay, respectively.

The central challenge lies in the evaluation of the strong transition amplitude $\langle BC, \mathbf{q} | \mathcal{H}_I | A \rangle$. This amplitude can be determined using the chiral quark model incorporating chiral dynamics, as outlined in previous works [30–35, 57–65].

In the chiral quark model, the low-energy quark-antiquark-pseudoscalar-meson interaction is described by the chiral Lagrangian: [60–62]:

$$\mathcal{L}_P = \sum_j \frac{1}{f_m} \bar{\psi}_j \gamma_\mu^j \gamma_5^j \psi_j \vec{\tau} \cdot \partial^\mu \vec{\phi}_m. \quad (4)$$

Here, ψ_j represents the j -th quark field in the hadron, ϕ_m is the pseudoscalar meson field, τ is an isospin operator, and f_m is the pseudoscalar meson decay constant.

By carrying out a nonrelativistic expansion of the chiral Lagrangian up to the mass order of $1/m^2$, one can obtain

$$\mathcal{H}_I = \mathcal{H}_I^{NR} + \mathcal{H}_I^{RC}, \quad (5)$$

where \mathcal{H}_I^{NR} is the nonrelativistic term at the order of $1/m$:

$$\mathcal{H}_I^{NR} = g \sum_j \left[\mathcal{G} \sigma_j \cdot \mathbf{q} + \frac{\omega_m}{2\mu_q} (\sigma_j \cdot \mathbf{p}_j) \right] I_j \varphi_m, \quad (6)$$

while \mathcal{H}_I^{RC} is the higher order term at the higher mass order of $1/m^2$, as a relativistic correction term of Eq. (6), which is given by

$$\begin{aligned} \mathcal{H}_I^{RC} = & -\frac{g}{32\mu_q^2} \sum_j [m_\pi^2 (\sigma_j \cdot \mathbf{q}) \\ & + 2\sigma_j \cdot (\mathbf{q} - 2\mathbf{p}_j) \times (\mathbf{q} \times \mathbf{p}_j)] I_j \varphi_m. \end{aligned} \quad (7)$$

In the above equations, \mathbf{p}_j and σ_j are the internal momentum operator and the spin operator of the j -th light quark in a hadron, respectively. $\varphi_m = e^{-i\mathbf{q}\cdot\mathbf{r}_j}$ is the plane wave part of the emitted light meson with three-vector momentum and energy denoted by (\mathbf{q}, ω_m) . m_π stands for the mass of the light pseudoscalar meson. I_j is an isospin operator defined in the SU(3) flavor space [61]. The factors g and \mathcal{G} are defined by $g \equiv \delta \sqrt{(E_i + M_i)(E_f + M_f)}/f_m$ and $\mathcal{G} \equiv -\left(1 + \frac{\omega_m}{E_f + M_f} + \frac{\omega_m}{2m'_j}\right)$, respectively, where $\delta = 0.557$ as a dimensionless strength parameter is determined by our previous works [31, 58], while the decay constants f_m for π , K and η are taken as $f_\pi = 132$ MeV, $f_K = f_\eta = 160$ MeV, respectively. E_i and M_i (E_f and M_f) are the energy and mass of the initial (final) heavy hadron, respectively. μ_q is defined by $1/\mu_q = 1/m_j + 1/m'_j$, where m_j and m'_j are the masses of the j -th light quark in the initial and final heavy hadrons, respectively.

It is noteworthy that \mathcal{H}_I^{RC} has often been overlooked in the existing literature [30–35, 58–62]. However, recent investigations into the strong decays of baryons [66, 67] have underscored the significance of \mathcal{H}_I^{RC} . This work signifies the inaugural inclusion of this term within the meson sector, and we will illustrate its pivotal role in accurately determining the widths of mesons. This effectively addresses the **P2** concern, especially the correct width, raised on the first page.

As we know the vertices described by \mathcal{H}_I are only effective in the non-perturbative region, which reflect the ability of $q\bar{q}$ creation in the vacuum. This ability will be suppressed in the high momentum region due to the weak interactions between the valence quarks. To suppress the nonphysical contributions in the high momentum region due to the hard vertices given

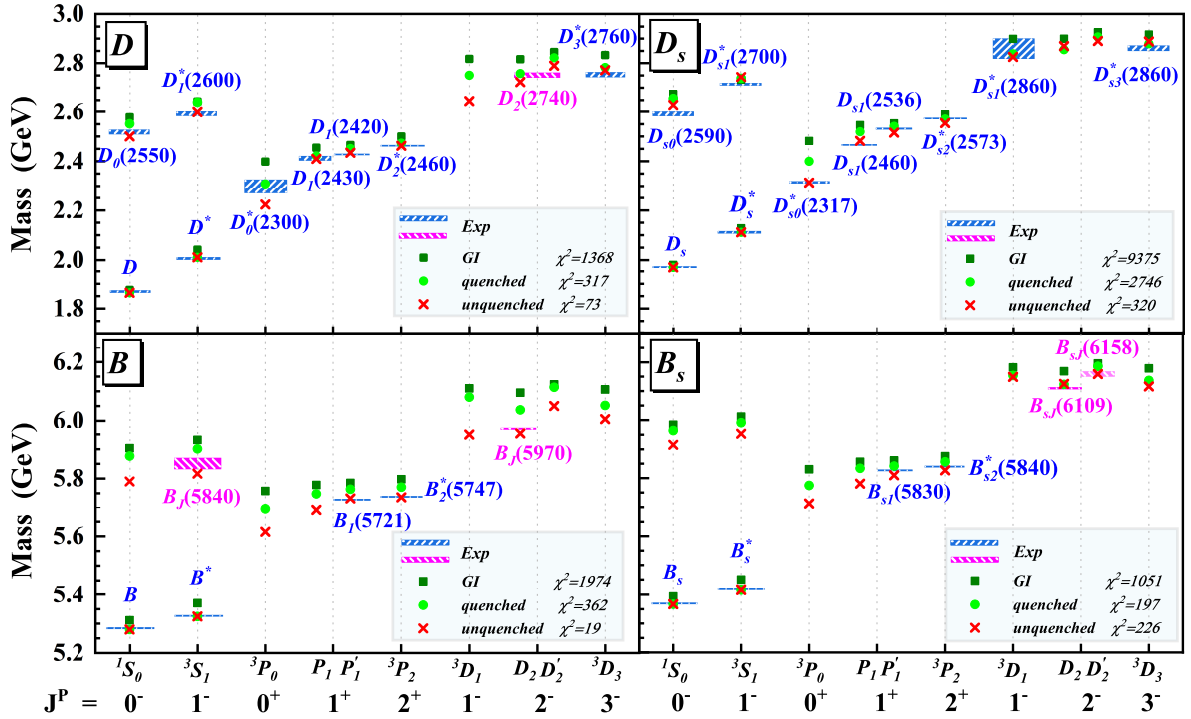


FIG. 1: Mass spectra of heavy-light mesons compared with the observations. The $\chi^2 = \sum_i (\text{Thy}(i) - \text{Exp}(i))^2 / \text{Error}(i)^2$ for the well-known GI model, our quenched model and unquenched spectrum, respectively. Here Thy, Exp and Error represent the theoretical results, experimental data and error, respectively. It should be noted that for data with experimental errors less than 1 MeV, we unified set Error = 2 MeV because our systemic error should be larger than several MeV.

by the chiral quark model, as indicated in **P3**, we incorporate a suppressed factor $e^{-q^2/(2\Lambda^2)}$ into the transition amplitude,

$$\langle BC, \mathbf{q} | \mathcal{H}_I | A \rangle \rightarrow \langle BC, \mathbf{q} | \mathcal{H}_I e^{-\frac{q^2}{2\Lambda^2}} | A \rangle, \quad (8)$$

as that done in the literature [68–73]. In this study, we employ a fixed cut-off parameter $\Lambda = 0.78$ GeV, which is comparable to the value of 0.84 GeV used in Refs. [70, 71]. We should emphasize that the application of suppressed factor is another crucial step for obtaining a successful description of the correct masses for the heavy-light mesons within a unified unquenched quark model as the **P2** concern. With this method, the mass corrections contributed by the higher partial wave couplings can be controlled.

Within this framework, we systematically address the significant issues **P1-P3** outlined on the first Page.

III. SPECTRUM

In Fig. 1, we present a comprehensive heavy-light meson spectrum across three distinct models alongside existing experimental data. The crossing points showing the spectrum including the coupled-channel effects are much closer to the experimental data than the results of other models. This improvement is further illustrated by the significant reduction in the magnitude of χ^2 , defined as $\sum_i (\text{Thy}(i) - \text{Exp}(i))^2 / \text{Error}(i)^2$. Based on these results, there is no doubt that the coupled chan-

nels play a key role in interpolating the spectra of the heavy-light mesons.

Firstly, the coupled-channel effects show their most significant influence on the 3P_0 and P_1 states. This is due to their coupling to S -wave interactions, involving a pseudo-scalar-heavy-meson and a vector-heavy-meson with a pseudo-scalar-light-meson for 3P_0 and P_1 states, respectively. For instance, there are strong interactions between $D_{s0}^*(2317)$ and DK , as well as between $D_{s1}(2460)$ and D^*K . These substantial coupled-channel effects naturally account for the significant mass shifts observed in these positive parity states. In contrast, the other two positive parity states, P_1' and 3P_2 , which involve D -wave interactions with the coupled channels, have minor mass shifts. This statement is consistent with recent work in Ref. [69]. The mass of $D_0^*(2300)$ with $J^P = 0^+$, which is approximately 2230 MeV in our results, is slightly lower than the experimental value of 2343 ± 10 MeV [6]. However, the mass of $D_0^*(2300)$ remains a subject of debate in various theoretical studies [74–78], primarily because its lineshape cannot be explained by the Breit-Wigner form used in the experimental analysis for extracting its mass. Notably, Lattice QCD calculations are consistent with our findings, where the complex pole position of D_0^* state is at $M - i\Gamma/2 = 2200 - i200$ MeV [79].

Secondly, the ground states of pseudo-scalars and vectors with $J^P = 0^-, 1^-$ exhibit minimal changes across all model for small couple channel effect, because their low mass forbid the decay channels except D^* which also has a very small

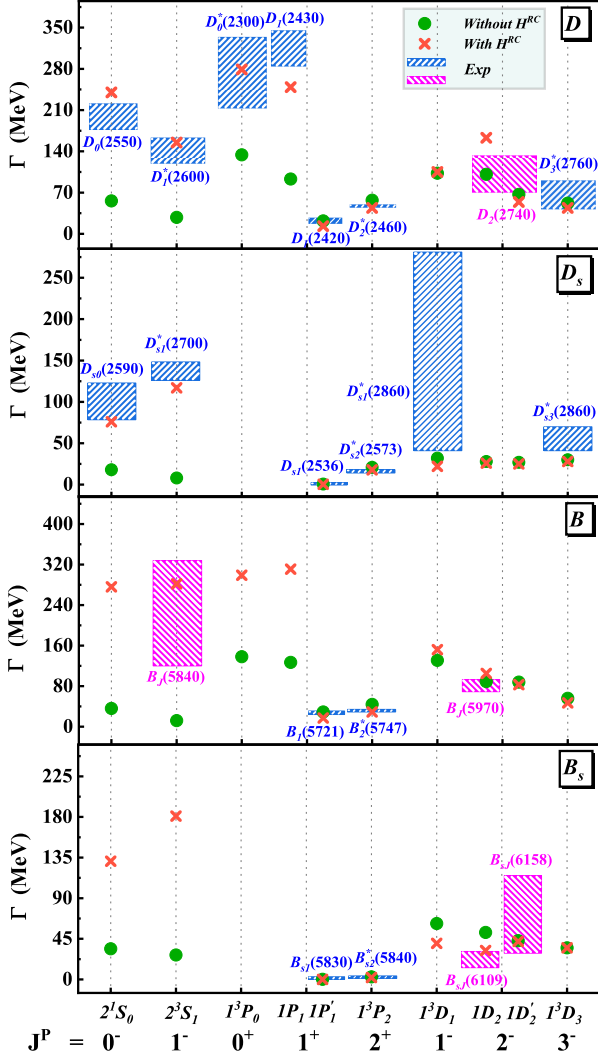


FIG. 2: Predictions of strong decay widths for the heavy-light mesons compared with the observations [6]. The cross (circular) symbol represents the predictions of the width with (without) the incorporation of the relativistic term \mathcal{H}_1^{RC} by combining unquenched spectra.

width. Conversely, the radial excited states have substantial mass shifts. The vector-heavy-meson and pseudo-scalar channels will be coupled with these excited states in P -wave, while for the D and B case, additional positive parity heavy-meson and pseudo-scalar channels can also be coupled with them in S -wave. Consequently, the mass shifts are even larger in the D and B cases.

Thirdly, let's consider $1D$ -wave heavy-light meson states. It is interesting to note that in the D_s and B_s sectors, the mass shifts are negligible, while they are significant in the D and B sectors. Actually, for the excited D_s and B_s states, pion production is prohibited due to isospin conservation in strong decay, while K meson is too heavy to effectively couple with positive parity excited D or B states in S -wave. As a result, for D_s and B_s sectors, the coupled-channel effects predominantly involve interactions with higher partial waves. In contrast,

S -wave channels remain available for D and B excited states when coupled with positive parity excited D and B states and pion. It is natural to interpolate the large mass shift in D and B sectors for $1D$ -wave states.

IV. WIDTHS

With the parameter set for the mass spectrum, we can compute the strong decay widths for all heavy-light meson resonances. In Fig. 2, we present the width values with and without \mathcal{H}_1^{RC} , represented by the red crossing and green circle points, respectively, as well as the experimental data. The widths of all well-established heavy-light meson states can be globally described well by including the relativistic correction term \mathcal{H}_1^{RC} .

For the radially excited states 2^1S_0 and 2^3S_1 across all heavy-light mesons, the widths enhance significantly by including \mathcal{H}_1^{RC} . This naturally addresses a long-standing puzzle, a broad-width of $D_0(2550)/D_{s0}(2590)$ and $D_1^*(2600)/D_{s1}^*(2700)$ in chiral quark model studies [31–35]. For $D_1^*(2600)$, the predicted partial width ratio $R_{th}^{D\pi/D^*\pi} = \Gamma(D\pi)/\Gamma(D^*\pi) \approx 0.34$ aligns well with the data $R_{exp}^{D\pi/D^*\pi} = 0.32 \pm 0.11$ [6]. Additionally, for the 3P_0 and P'_1 in D and B sectors, the widths also exhibit increasing, which leads to the predicted widths of $D_0^*(2300)$ and $D_1(2430)$ are both closer to the observations. These enhancements can be attributed to the second term of \mathcal{H}_1^{RC} , where even powers of quark momentum strengthen the transition, while all other odd-power momentum operators cancel each other [66, 67].

V. PREDICTION

We have demonstrated that our innovative model successfully describes the masses and widths of existing heavy-light mesons. To further examine our model, we also provide predictions for various masses and widths for heavy-light mesons. Upon the confirmation of these states, our understanding of the structure of hadrons will be significantly enriched. Additionally, we provide the main decay ratios of these states in Fig. 3.

For the charmed meson, from Fig. 1, two 3D_1 and D'_2 states for D meson and two D_2 states in D_s sector are all unobserved in the experiments. These states exhibit narrow widths as illustrated in Fig. 2. In our model, we also provide the decay rates for these predicted states, as depicted in Fig. 3. Notably, for 3D_1 D state, the primary decay channel with the widest width is $D_1(2420)\pi$. This decay mode offers a valuable final state for experimental searches targeting this state.

On the other hand, several excited states of B and B_s mesons remain unobserved, with notable examples being the 3P_0 and P'_1 states of B and B_s . In our model, we predict the masses of $B(1^3P_0)$ and $B(1P_1)$ to be 5616 MeV and 5691 MeV, respectively, which is consistent with those in Refs. [78, 80, 81], while $B_s(1^3P_0)$ and $B_s(1P_1)$ are predicted to be 5711 MeV and 5781 MeV here, which are in good agreement with those

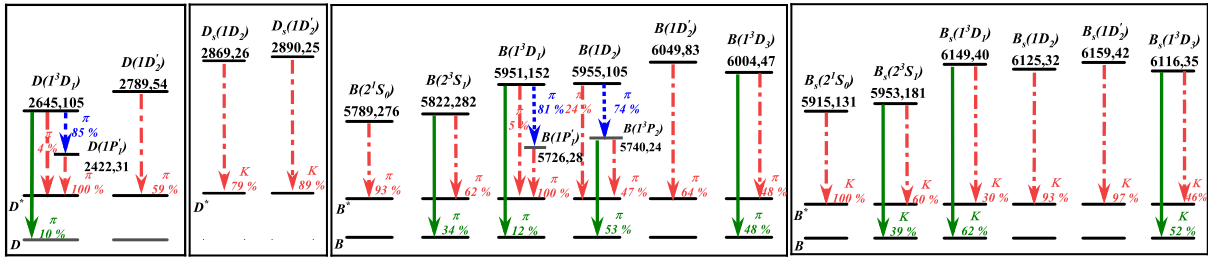


FIG. 3: Predictions of decay rates of the main decay channels for the missing states in the D , D_s , B , and B_s families. The values located below the meson state represent the predicted mass and strong decay width in MeV units.

from Lattice QCD [82, 83] and other coupled-channel models [71, 72, 84–88]. It strengthens the reliability of our model, and the widths of them are also predicted. As shown in Fig. 3, the main decay channels of $B(1^3P_0)$ and $B(1P_1)$ are $B\pi$ and $B^*\pi$, respectively, while $B_s(1^3P_0)$ and $B_s(1P_1)$ should be both narrow states which is similar as $D_{s0}^*(2317)$ and $D_{s1}(2460)$.

Additionally, numerous negative parity beauty mesons remain to be discovered in experimental searches. We would like to highlight a few notable cases. By comparing with the masses, we find that the $B_J(5840)$ favors the 2^3S_1 state, which is consistent with the assignment in Ref. [89]. The partial width ratio $\Gamma(B\pi)/\Gamma(B^*\pi) \simeq 0.55$ can be subject to verification in future experiments. The newly observed structures, $B_{sJ}(6064)$ and $B_{sJ}(6114)$, in the B^+K^- mass spectrum at LHCb [90], may potentially be explained by the presence of $B_s(1^3D_3)$ and $B_s(1^3D_1)$ states. Their primary predicted decay channel is B^+K^- . In addition, these two structures could also be caused by higher mass resonances $B_{sJ}(6109)$ and $B_{sJ}(6158)$, respectively, which mainly decay into $B^{*+}K^-$.

VI. SUMMARY

In this study, we propose a unified unquenched quark model framework, which for the first time successfully provides comprehensive mass spectra, decay widths, and strong decay branch widths for the D , D_s , B , and B_s sectors. This unquenched quark model not only combines the traditional quark model and the coupled-channel effects based on chiral dynamics, but also incorporates a relativistic correction

term for describing the strong transition amplitude for the first time. These theoretical approaches and strategies adopted in the present work ensure that our model is excellent for simultaneously describing the masses and decay widths of all existing heavy-light mesons.

Notably, our model naturally resolves the long-standing puzzles that the low-mass nature of $D_{s0}^*(2317)$ and $D_{s1}(2460)$ and the broad nature of radial excitations $D_0(2550)/D_{s0}(2590)$ and $D_1^*(2600)/D_{s1}^*(2700)$. Furthermore, our model predicts the masses, widths, and branching ratios of various new states, offering valuable guidance for their discovery in future experiments. Some of our predictions are consistent with the lattice data, strengthening our confidence in extending this model to the other hadron spectra, such as the light baryon spectrum and singly-heavy baryon spectrum. The success of the unquenched quark model presented in this work indicates it may be an important step for understanding the hadron spectrum.

Acknowledgements

We thank useful discussions from Qiang Zhao, Xiang Liu, Zhi-Yong Zhou, and A. J. Arifi. This work is supported by the National Natural Science Foundation of China under Grants Nos.12175065 and 12235018 (X.H.Z), 12175239 and 12221005 (J.J.W), and by the National Key R & D Program of China under Contract No. 2020YFA0406400 (J.J.W), and supported by Chinese Academy of Sciences under Grant No. YSBR-101 (J.J.W).

-
- [1] M. Gell-Mann, A Schematic Model of Baryons and Mesons, Phys. Lett. **8**, 214-215 (1964).
 - [2] G. Zweig, An SU(3) model for strong interaction symmetry and its breaking. Version 1, CERN-TH-401.
 - [3] G. Zweig, An SU(3) model for strong interaction symmetry and its breaking. Version 2, CERN-TH-412.
 - [4] S. K. Choi *et al.* [Belle], Observation of a narrow charmonium-like state in exclusive $B^{\pm} \rightarrow K^{\pm}\pi^{\pm}\pi^{\mp}J/\psi$ decays, Phys. Rev. Lett. **91**, 262001 (2003).
 - [5] B. Aubert *et al.* [BaBar], Observation of a narrow meson decaying to $D_s^+\pi^0$ at a mass of 2.32-GeV/c², Phys. Rev. Lett. **90**, 242001 (2003).
 - [6] R. L. Workman *et al.* [Particle Data Group], Review of Particle Physics, PTEP **2022**, 083C01 (2022).
 - [7] S. Capstick and N. Isgur, Baryons in a relativized quark model with chromodynamics, Phys. Rev. D **34**, no.9, 2809-2835 (1986).
 - [8] E. Eichten, K. Gottfried, T. Kinoshita, K. D. Lane and T. M. Yan, Charmonium: The Model, Phys. Rev. D **17**, 3090 (1978) [erratum: Phys. Rev. D **21**, 313 (1980)].
 - [9] S. Godfrey and N. Isgur, Mesons in a Relativized Quark Model with Chromodynamics, Phys. Rev. D **32**, 189-231 (1985).
 - [10] T. Barnes, S. Godfrey, and E. S. Swanson, Higher charmonia, Phys. Rev. D **72**, 054026 (2005).

- [11] J. Zeng, J. W. Van Orden and W. Roberts, Heavy mesons in a relativistic model, *Phys. Rev. D* **52**, 5229-5241 (1995).
- [12] J. Vijande, F. Fernandez and A. Valcarce, Constituent quark model study of the meson spectra, *J. Phys. G* **31**, 481 (2005).
- [13] D. Ebert, R. N. Faustov and V. O. Galkin, Heavy-light meson spectroscopy and Regge trajectories in the relativistic quark model, *Eur. Phys. J. C* **66**, 197-206 (2010).
- [14] J. B. Liu and M. Z. Yang, Spectrum of the charmed and b-flavored mesons in the relativistic potential model, *JHEP* **07**, 106 (2014).
- [15] J. B. Liu and C. D. Lu, Spectra of heavy-light mesons in a relativistic model, *Eur. Phys. J. C* **77**, no.5, 312 (2017).
- [16] J. B. Liu and M. Z. Yang, Spectrum of Higher excitations of B and D mesons in the relativistic potential model, *Phys. Rev. D* **91**, no.9, 094004 (2015).
- [17] D. Ebert, V. O. Galkin and R. N. Faustov, Mass spectrum of orbitally and radially excited heavy-light mesons in the relativistic quark model, *Phys. Rev. D* **57**, 5663-5669 (1998) [erratum: *Phys. Rev. D* **59**, 019902 (1999)].
- [18] W. J. Deng, H. Liu, L. C. Gui and X. H. Zhong, Spectrum and electromagnetic transitions of bottomonium, *Phys. Rev. D* **95**, no.7, 074002 (2017).
- [19] W. J. Deng, H. Liu, L. C. Gui and X. H. Zhong, Charmonium spectrum and their electromagnetic transitions with higher multipole contributions, *Phys. Rev. D* **95**, no.3, 034026 (2017).
- [20] S. Godfrey and K. Moats, Properties of Excited Charm and Charm-Strange Mesons, *Phys. Rev. D* **93**, no.3, 034035 (2016).
- [21] S. Godfrey, K. Moats and E. S. Swanson, B and B_s Meson Spectroscopy, *Phys. Rev. D* **94**, 054025 (2016).
- [22] I. Asghar, B. Masud, E. S. Swanson, F. Akram and M. Atif Sultan, Decays and spectrum of bottom and bottom strange mesons, *Eur. Phys. J. A* **54**, no.7, 127 (2018).
- [23] D. M. Li, P. F. Ji and B. Ma, The newly observed open-charm states in quark model, *Eur. Phys. J. C* **71**, 1582 (2011).
- [24] Q. F. Lü, T. T. Pan, Y. Y. Wang, E. Wang and D. M. Li, Excited bottom and bottom-strange mesons in the quark model, *Phys. Rev. D* **94**, no.7, 074012 (2016).
- [25] P. Colangelo, F. De Fazio, F. Giannuzzi and S. Nicotri, New meson spectroscopy with open charm and beauty, *Phys. Rev. D* **86**, 054024 (2012).
- [26] Y. Sun, Q. T. Song, D. Y. Chen, X. Liu and S. L. Zhu, Higher bottom and bottom-strange mesons, *Phys. Rev. D* **89**, 054026 (2014).
- [27] Q. T. Song, D. Y. Chen, X. Liu and T. Matsuki, Higher radial and orbital excitations in the charmed meson family, *Phys. Rev. D* **92**, no.7, 074011 (2015).
- [28] Q. T. Song, D. Y. Chen, X. Liu and T. Matsuki, Charmed-strange mesons revisited: mass spectra and strong decays, *Phys. Rev. D* **91**, 054031 (2015).
- [29] J. Ferretti and E. Santopinto, Open-flavor strong decays of open-charm and open-bottom mesons in the 3P_0 model, *Phys. Rev. D* **97**, no.11, 114020 (2018).
- [30] M. Di Pierro and E. Eichten, Excited Heavy-Light Systems and Hadronic Transitions, *Phys. Rev. D* **64**, 114004 (2001).
- [31] X. H. Zhong and Q. Zhao, Strong decays of heavy-light mesons in a chiral quark model, *Phys. Rev. D* **78**, 014029 (2008).
- [32] X. H. Zhong and Q. Zhao, Strong decays of newly observed D_{sJ} states in a constituent quark model with effective Lagrangians, *Phys. Rev. D* **81**, 014031 (2010).
- [33] X. H. Zhong, Strong decays of the newly observed $D(2550)$, $D(2600)$, $D(2750)$, and $D(2760)$, *Phys. Rev. D* **82**, 114014 (2010).
- [34] L. Y. Xiao and X. H. Zhong, Strong decays of higher excited heavy-light mesons in a chiral quark model, *Phys. Rev. D* **90**, no.7, 074029 (2014).
- [35] R. H. Ni, Q. Li and X. H. Zhong, Mass spectra and strong decays of charmed and charmed-strange mesons, *Phys. Rev. D* **105**, no.5, 056006 (2022).
- [36] S. Capstick and W. Roberts, Quark models of baryon masses and decays, *Prog. Part. Nucl. Phys.* **45**, S241-S331 (2000).
- [37] H. X. Chen, W. Chen, X. Liu, Y. R. Liu and S. L. Zhu, A review of the open charm and open bottom systems, *Rept. Prog. Phys.* **80**, no.7, 076201 (2017).
- [38] H. X. Chen, W. Chen, X. Liu, Y. R. Liu and S. L. Zhu, An updated review of the new hadron states, *Rept. Prog. Phys.* **86**, no.2, 026201 (2023).
- [39] S. Theberge, A. W. Thomas and G. A. Miller, The Cloudy Bag Model. 1. The (3,3) Resonance, *Phys. Rev. D* **22**, 2838 (1980) [erratum: *Phys. Rev. D* **23**, 2106 (1981)].
- [40] D. S. Hwang and D. W. Kim, Mass of D_{sJ}^* (2317) and coupled channel effect, *Phys. Lett. B* **601**, 137 (2004).
- [41] Y. B. Dai, C. S. Huang, C. Liu and S. L. Zhu, Understanding the D_{sJ}^+ (2317) and D_{sJ}^+ (2460) with sum rules in HQET, *Phys. Rev. D* **68**, 114011 (2003).
- [42] Z. Y. Zhou and Z. Xiao, Two-pole structures in a relativistic Friedrichs-Lee-QPC scheme, *Eur. Phys. J. C* **81** (2021) no.6, 551.
- [43] X. G. Wu and Q. Zhao, The mixing of D_{s1} (2460) and D_{s1} (2536), *Phys. Rev. D* **85**, 034040 (2012).
- [44] D. Mohler, C. B. Lang, L. Leskovec, S. Prelovsek and R. M. Woloshyn, D_{s0}^* (2317) Meson and D -Meson-Kaon Scattering from Lattice QCD, *Phys. Rev. Lett.* **111**, no.22, 222001 (2013).
- [45] C. B. Lang, L. Leskovec, D. Mohler, S. Prelovsek and R. M. Woloshyn, D_s mesons with DK and D^*K scattering near threshold, *Phys. Rev. D* **90**, no.3, 034510 (2014).
- [46] Z. Y. Zhou and Z. Xiao, Hadron loops effect on mass shifts of the charmed and charmed-strange spectra, *Phys. Rev. D* **84**, 034023 (2011).
- [47] J. M. Xie, M. Z. Liu and L. S. Geng, D_{s0} (2590) as a dominant $c\bar{s}$ state with a small D^*K component, *Phys. Rev. D* **104**, no.9, 094051 (2021).
- [48] W. Hao, Y. Lu and B. S. Zou, Coupled channel effects for the charmed-strange mesons, *Phys. Rev. D* **106**, no.7, 074014 (2022).
- [49] K. Heikkilä, S. Ono and N. A. Tornqvist, HEAVY $c\bar{c}$ AND $b\bar{b}$ QUARKONIUM STATES AND UNITARITY EFFECTS, *Phys. Rev. D* **29**, 110 (1984) [erratum: *Phys. Rev. D* **29**, 2136 (1984)].
- [50] Y. S. Kalashnikova, Coupled-channel model for charmonium levels and an option for $X(3872)$, *Phys. Rev. D* **72**, 034010 (2005).
- [51] T. Barnes and E. S. Swanson, Hadron loops: General theorems and application to charmonium, *Phys. Rev. C* **77**, 055206 (2008).
- [52] Y. Lu, M. N. Anwar and B. S. Zou, Coupled-Channel Effects for the Bottomonium with Realistic Wave Functions, *Phys. Rev. D* **94**, no.3, 034021 (2016).
- [53] P. G. Ortega, J. Segovia, D. R. Entem and F. Fernandez, Coupled channel approach to the structure of the $X(3872)$, *Phys. Rev. D* **81**, 054023 (2010).
- [54] See the supplementary material accessible through the journal webpage for further details of the model and numerical calculation results.
- [55] M. R. Pennington and D. J. Wilson, Decay channels and charmonium mass-shifts, *Phys. Rev. D* **76**, 077502 (2007).
- [56] M. X. Duan and X. Liu, Where are 3P and higher P-wave states in the charmonium family?, *Phys. Rev. D* **104**, no.7, 074010

- (2021).
- [57] A. Manohar and H. Georgi, Chiral Quarks and the Nonrelativistic Quark Model, Nucl. Phys. B **234**, 189-212 (1984).
- [58] X. H. Zhong and Q. Zhao, Charmed baryon strong decays in a chiral quark model, Phys. Rev. D **77**, 074008 (2008).
- [59] Q. li, R. H. Ni and X. H. Zhong, Towards establishing an abundant B and B_s spectrum up to the second orbital excitations, Phys. Rev. D **103**, 116010 (2021).
- [60] Z. P. Li, The Threshold pion photoproduction of nucleons in the chiral quark model, Phys. Rev. D **50**, 5639-5646 (1994).
- [61] Z. P. Li, H. X. Ye and M. H. Lu, An Unified approach to pseudoscalar meson photoproductions off nucleons in the quark model, Phys. Rev. C **56**, 1099-1113 (1997).
- [62] Q. Zhao, J. S. Al-Khalili, Z. P. Li and R. L. Workman, Pion photoproduction on the nucleon in the quark model, Phys. Rev. C **65**, 065204 (2002).
- [63] Q. Zhao, Z. P. Li and C. Bennhold, Vector meson photoproduction with an effective Lagrangian in the quark model, Phys. Rev. C **58**, 2393-2413 (1998).
- [64] Q. Zhao, Nucleonic resonance excitations with linearly polarized photon in $\gamma p \rightarrow \omega p$, Phys. Rev. C **63**, 025203 (2001).
- [65] Q. Zhao, J. S. Al-Khalili and C. Bennhold, Quark model predictions for K^* photoproduction on the proton, Phys. Rev. C **64**, 052201 (2001).
- [66] A. J. Arifi, D. Suenaga and A. Hosaka, Relativistic corrections to decays of heavy baryons in the quark model, Phys. Rev. D **103**, no.9, 094003 (2021).
- [67] A. J. Arifi, D. Suenaga, A. Hosaka and Y. Oh, Strong decays of multistrangeness baryon resonances in the quark model, Phys. Rev. D **105**, no.9, 094006 (2022).
- [68] B. Silvestre- Brac and C. Gignoux, Unitary effects in spin orbit splitting of P wave baryons, Phys. Rev. D **43**, 3699-3708 (1991).
- [69] Z. Yang, G. J. Wang, J. J. Wu, M. Oka and S. L. Zhu, Novel Coupled Channel Framework Connecting the Quark Model and Lattice QCD for the Near-threshold Ds States, Phys. Rev. Lett. **128**, no.11, 11 (2022).
- [70] P. G. Ortega, J. Segovia, D. R. Entem and F. Fernandez, Molecular components in P-wave charmed-strange mesons, Phys. Rev. D **94**, no.7, 074037 (2016).
- [71] P. G. Ortega, J. Segovia, D. R. Entem and F. Fernández, Threshold effects in P-wave bottom-strange mesons, Phys. Rev. D **95**, no.3, 034010 (2017).
- [72] Z. Yang, G. J. Wang, J. J. Wu, M. Oka and S. L. Zhu, The investigations of the P-wave B_s states combining quark model and lattice QCD in the coupled channel framework, JHEP **01**, 058 (2023).
- [73] H. H. Zhong, R. H. Ni, M. Y. Chen, X. H. Zhong and J. J. Xie, Further study of $\Omega^* |1P_{3/2^-}\rangle$ within a chiral quark model, Chin. Phys. C **47**, no.6, 063104 (2023).
- [74] E. van Beveren and G. Rupp, Observed $D_s(2317)$ and tentative $D(2100-2300)$ as the charmed cousins of the light scalar nonet, Phys. Rev. Lett. **91**, 012003 (2003).
- [75] M. Albaladejo, P. Fernandez-Soler, F. K. Guo and J. Nieves, Two-pole structure of the $D_0^*(2400)$, Phys. Lett. B **767**, 465-469 (2017).
- [76] M. L. Du, M. Albaladejo, P. Fernández-Soler, F. K. Guo, C. Hanhart, U. G. Meißner, J. Nieves and D. L. Yao, Towards a new paradigm for heavy-light meson spectroscopy, Phys. Rev. D **98**, no.9, 094018 (2018).
- [77] M. L. Du, F. K. Guo, C. Hanhart, B. Kubis and U. G. Meißner, Where is the lightest charmed scalar meson?, Phys. Rev. Lett. **126**, no.19, 192001 (2021).
- [78] W. A. Bardeen, E. J. Eichten and C. T. Hill, Chiral multiplets of heavy - light mesons, Phys. Rev. D **68**, 054024 (2003).
- [79] L. Gayer *et al.* [Hadron Spectrum], Isospin-1/2 $D\pi$ scattering and the lightest D_0^* resonance from lattice QCD, JHEP **07**, 123 (2021).
- [80] I. Woo Lee and T. Lee, Why there is no spin-orbit inversion in heavy-light mesons?, Phys. Rev. D **76**, 014017 (2007).
- [81] J. Vijande, A. Valcarce and F. Fernandez, B meson spectroscopy, Phys. Rev. D **77**, 017501 (2008).
- [82] C. B. Lang, D. Mohler, S. Prelovsek and R. M. Woloshyn, Predicting positive parity B_s mesons from lattice QCD, Phys. Lett. B **750**, 17-21 (2015).
- [83] E. B. Gregory, C. T. H. Davies, I. D. Kendall, J. Koponen, K. Wong, E. Follana, E. Gamiz, G. P. Lepage, E. H. Muller and H. Na, *et al.* Precise B , B_s and B_c meson spectroscopy from full lattice QCD, Phys. Rev. D **83**, 014506 (2011).
- [84] H. Y. Cheng and F. S. Yu, Near mass degeneracy in the scalar meson sector: Implications for $B_{(s)0}^*$ and $B'_{(s)1}$ mesons, Phys. Rev. D **89**, no.11, 114017 (2014).
- [85] H. Y. Cheng and F. S. Yu, Masses of Scalar and Axial-Vector B Mesons Revisited, Eur. Phys. J. C **77**, no.10, 668 (2017).
- [86] M. Albaladejo, P. Fernandez-Soler, J. Nieves and P. G. Ortega, Lowest-lying even-parity \bar{B}_s mesons: heavy-quark spin-flavor symmetry, chiral dynamics, and constituent quark-model bare masses, Eur. Phys. J. C **77**, no.3, 170 (2017).
- [87] F. K. Guo, P. N. Shen and H. C. Chiang, Dynamically generated 1^+ heavy mesons, Phys. Lett. B **647**, 133 (2007).
- [88] F. K. Guo, P. N. Shen, H. C. Chiang, R. G. Ping and B. S. Zou, Dynamically generated 0^+ heavy mesons in a heavy chiral unitary approach, Phys. Lett. B **641**, 278 (2006).
- [89] G. L. Yu and Z. G. Wang, Analysis of the excited bottom and bottom-strange states $B_1(5721)$, $B_2^*(5747)$, $B_{s1}(5830)$, $B_{s2}^*(5840)$, $B_J(5840)$ and $B_J(5970)$ in B meson family, Chin. Phys. C **44**, no.3, 033103 (2020).
- [90] R. Aaij *et al.* [LHCb], Observation of new excited B_s^0 states, Eur. Phys. J. C **81**, 601 (2021).
- [91] E. Hiyama, Y. Kino and M. Kamimura, Gaussian expansion method for few-body systems, Prog. Part. Nucl. Phys. **51**, 223-307 (2003).

Supplemental Material

1. Potential model

The bare mass and numerical wave functions of the heavy-light meson are calculate by a semirelativistic potential quark model. In the model, the effective Hamiltonian is given by

$$\mathcal{H}_0 = \sqrt{\mathbf{p}_1^2 + m_1^2} + \sqrt{\mathbf{p}_2^2 + m_2^2} + V(r), \quad (9)$$

where the first two terms stand for the kinetic energies for the light antiquark \bar{q} and heavy quark Q , respectively, $V(r)$ stands for the effective potentials between two quarks, which is given by

$$V(r) = V_0(r) + V_{sd}(r). \quad (10)$$

Here $V_0(r)$ is the well-known Cornell potential [8]

$$V_0(r) = -\frac{4}{3} \frac{\alpha_s(r)}{r} + br + C_0, \quad (11)$$

which includes the color Coulomb interaction and linear confinement, and zero point energy C_0 . The $V_{sd}(r)$ is the spin-dependent part, we adopted the widely used form [9, 10]

$$V_{sd}(r) = \frac{32\pi\alpha_s(r) \cdot \sigma^3 e^{-\sigma^2 r^2}}{9\sqrt{\pi}\tilde{m}_1 m_2} \mathbf{S}_1 \cdot \mathbf{S}_2 + \frac{4}{3} \frac{\alpha_s(r)}{\tilde{m}_1 m_2} \frac{1}{r^3} \left(\frac{3\mathbf{S}_1 \cdot \mathbf{r} \mathbf{S}_2 \cdot \mathbf{r}}{r^2} - \mathbf{S}_1 \cdot \mathbf{S}_2 \right) + H_{LS}. \quad (12)$$

In the Eq. (12), the first term is the spin-spin contact hyperfine potential, the second term is the tensor potential, the H_{LS} stands for the spin-orbit interaction, which can be decomposed into symmetric part H_{sym} and antisymmetric part H_{anti} :

$$H_{sym} = \frac{\mathbf{S}_+ \cdot \mathbf{L}}{2} \left[\left(\frac{1}{2\tilde{m}_1^2} + \frac{1}{2m_2^2} \right) \left(\frac{4\alpha_s(r)}{3r^3} - \frac{b}{r} \right) + \frac{8\alpha_s(r)}{3\tilde{m}_1 m_2 r^3} \right] \quad (13)$$

$$H_{anti} = \frac{\mathbf{S}_- \cdot \mathbf{L}}{2} \left(\frac{1}{2\tilde{m}_1^2} - \frac{1}{2m_2^2} \right) \left(\frac{4\alpha_s(r)}{3r^3} - \frac{b}{r} \right). \quad (14)$$

In these equations, \mathbf{L} is the relative orbital angular momentum of the $Q\bar{q}$ system; \mathbf{S}_1 and \mathbf{S}_2 are the spins of the light and heavy quarks, respectively, and $\mathbf{S}_\pm \equiv \mathbf{S}_1 \pm \mathbf{S}_2$.

The antisymmetric part of the spin-orbit interaction, H_{anti} , can cause a configuration mixing between spin-triplet n^3L_J and spin-singlet n^1L_J for the $Q\bar{q}$ system. Thus, the physical states nL_J and nL'_J are expressed as

$$\begin{pmatrix} nL_J \\ nL'_J \end{pmatrix} = \begin{pmatrix} \cos \theta_{nL} & \sin \theta_{nL} \\ -\sin \theta_{nL} & \cos \theta_{nL} \end{pmatrix} \begin{pmatrix} n^1L_J \\ n^3L_J \end{pmatrix}, \quad (15)$$

where $J = L = 1, 2, 3 \dots$, and the θ_{nL} is the mixing angle. In this work, nL_J and nL'_J correspond to the lower-mass and higher-mass mixed states, respectively, as often adopted in the literature. This mixing angle can be perturbatively determined with the nondiagonal matrix element $\langle n^1L_J | \mathcal{H}_{anti} | n^3L_J \rangle$.

The running coupling constant $\alpha_s(r)$ adopted a parameterized form, $\alpha_s(r) = \sum_{i=1,2,3} \alpha_i \frac{2}{\sqrt{\pi}} \int_0^{\gamma_i r} e^{-x^2} dx$, in the coordinate space. In the different heavy-light meson systems, we set the consistent parameters $\alpha_2 = 0.15$, $\alpha_3 = 0.20$, $\gamma_1 = 1/2$, $\gamma_2 = \sqrt{10}/2$, and $\gamma_3 = \sqrt{1000}/2$, which are the same as those adopted in Refs. [9, 14, 16]. The parameter α_1 is slightly different for $D_{(s)}$ and $B_{(s)}$ spectra for a better description the mass spectrum, as shown in the value in Table I. It should be mentioned that in the spin-dependent potentials, we have replaced the light quark mass m_1 with \tilde{m}_1 to include some relativistic corrections. By using the Gaussian expansion method [91] to solve the Schrödinger equation, the bare mass and numerical wave functions for heavy-light mesons are derived. Detailed discussions on the numerical calculation techniques involving Gaussian expansion can be found in our previous work [35].

2. Model parameters

In the quark potential model, the slope parameter b for the linear potential is taken to be $b = 0.18 \text{ GeV}^2$, which is a typical value adopted in various relativistic potential models [9, 11, 17]. The other parameters,

$\{\alpha_1, \sigma, C_0, m_c, m_b, m_{u/d}, m_s, \tilde{m}_{u/d}, \tilde{m}_s, r_c\}$, are determined by fitting the low-lying well-established states. To overcome the singular behavior of $1/r^3$ in the spin-dependent potentials, we introduce a cutoff distance r_c in the calculation, which allows $1/r^3 = 1/r_c^3$ within a small range $r \in (0, r_c)$, as we did in the previous studies [18, 19, 35, 59]. In this work, we give two solutions for the heavy-light meson spectrum. One solution is obtained within the quenched quark model without coupled-channel effects, and the other one is obtained within the unquenched quark model with coupled-channel effects. The parameter sets have been listed in Table I. For the calculation of the strong transition amplitude $\langle BC, \mathbf{q} | \mathcal{H}_I | A \rangle$ within the chiral quark model, one can find that the relativistic correction term \mathcal{H}_I^{RC} is sensitive to the effective mass of the light u/d quarks due to the factor $1/\mu_q^2 = (1/m_j + 1/m'_j)^2$. Thus, to obtain a good description of the strong decay properties and coupled-channel effects for the heavy-light meson states, the effective mass of the u/d quark is taken to be $m_u = m_d = 0.45 \text{ GeV}$, which is slightly larger than that used in the potential model for the study of the mass spectrum. In fact, the operator \mathcal{H}_I is derived from the effective Lagrangians through a weak binding approximation, the interaction between the quarks is not seriously considered as that in the potential model. Thus, the effective u/d quark mass in the chiral quark model should be slightly different from that in the potential model.

Furthermore, to obtain the transition amplitude $\langle BC, \mathbf{q} | \mathcal{H}_I | A \rangle$, we adopt the numerical wave functions for the heavy-light mesons, except the ground states $D^{(*)}$ and $B^{(*)}$. We have noted that the decays of most excited heavy-light states are related to the ground states, their transition amplitudes are sensitive to the details of the wave functions of the ground states $D^{(*)}$ and $B^{(*)}$. Considering the uncertainty of the ground state wave functions, we properly adjust their size to more reasonably describe the strong decay properties of the well-established states, such as $D_2^*(2460)$, $D_{s2}^*(2573)$, $B_2^*(5747)$, and $B_{s2}^*(5840)$. For convenience, the ground wave functions are adopted a simple harmonic oscillator form with an effective size parameter β_{eff} . The determined β_{eff} parameters for $D^{(*)}$ and $B^{(*)}$ have been listed in Table II. There is about a 10% correction to the effective β_{eff} parameters which are extracted from the numerical wave functions of $D^{(*)}$ and $B^{(*)}$ by reproducing the root-mean-square radius $\sqrt{\langle r^2 \rangle}$ with a simple harmonic oscillator form.

3. More details of numerical results

The masses for the heavy-light meson states obtained from the quenched and unquenched quark models are listed in Table III. The decay widths of the heavy-light meson from the two methods are also listed in Table III. In method I, the decay widths are described without relativistic correction term \mathcal{H}_I^{RC} by combining the spectrum from the unquenched quark model. While in method II, the decay widths are described with relativistic correction term \mathcal{H}_I^{RC} by combining the spectrum also from the unquenched quark model. It is found that with relativistic correction of the descriptions of the decay

TABLE I: Potential model parameters for quenched and unquenched mass spectra.

	$m_{c/b}(\text{GeV})$	$m_{u,d}(\text{GeV})$	$\tilde{m}_{u,d}(\text{GeV})$	$m_s(\text{GeV})$	$\tilde{m}_s(\text{GeV})$	α_1	$b(\text{GeV}^2)$	$\sigma(\text{GeV})$	$C_0(\text{MeV})$	$r_c(\text{fm})$
<i>quenched</i>										
D	1.45	0.45	0.64	0.28	0.180	0.953	-302.0	0.332
D_s	1.45	0.55	0.70	0.28	0.180	0.990	-267.0	0.320
B	4.80	0.45	0.64	0.22	0.180	0.870	-246.0	0.266
B_s	4.80	0.55	0.70	0.22	0.180	0.965	-218.0	0.253
<i>unquenched</i>										
D	1.45	0.35	0.64	0.38	0.180	0.930	-179.0	0.341
D_s	1.45	0.55	0.70	0.38	0.180	0.882	-212.0	0.325
B	4.80	0.35	0.64	0.25	0.180	0.870	-172.0	0.270
B_s	4.80	0.55	0.70	0.25	0.180	0.939	-200.0	0.256

TABLE II: The effective β_{eff} (GeV) parameters for the ground states $D^{(*)}$ and $B^{(*)}$ in the quenched/unquenched pictures. In the table, β_{eff}^A stands for the results determined by the strong decay properties of the well-established heavy-light states, while β_{eff}^B stands for the results extracted from the numerical wave functions the ground states $D^{(*)}$ and $B^{(*)}$ obtained in the potential model.

	D	D^*	B	B^*
β_{eff}^A	0.499/0.497	0.454/0.449	0.524/0.509	0.512/0.498
β_{eff}^B	0.587/0.585	0.493/0.488	0.616/0.599	0.582/0.566

widths for the heavy-light states have an overall improvement.

In Tables IV and V, the mass shifts, and partial widths of the heavy light meson states contributed by each channel are given. From the tables, one can find which channels play a crucial role in the mass shift of a heavy-light meson, and which channels dominate their strong decays. One also can see the details of the relativistic corrections to the partial widths of each channel. The partial width ratios between different decay channels and their branching fractions for each state can be obtained from these tables.

TABLE III: Theoretical masses and widths compared with the data. The mass spectra from both the quenched and unquenched pictures are given, which are denoted with Q and UQ , respectively. The strong decay widths, which combine the unquenched spectra and are described by non-relativistic chiral interactions \mathcal{H}_i^{NR} , are further augmented by a relativistic correction term \mathcal{H}_i^{RC} . These widths are denoted as Γ_i^{NR} and Γ_i^{NR+RC} , respectively. The experimental data are taken from the PDG [6]. The mixing angles for $1P_1/1P_1'$ states in the D , D_s , B and B_s families are determined to be -30.0° , -26.5° , -34.3° , and -34.2° , respectively. While the mixing angles for $1D_2/1D_2'$ states in the D , D_s , B and B_s families are determined to be -40.5° , -40.5° , -39.9° , and -40.2° , respectively.

		<i>D mesons</i>						<i>D_s mesons</i>						
$n^{2S+1}L_J$	Observed state	Mass (MeV)			Width (MeV)			Observed state	Mass (MeV)			Width (MeV)		
		Q	UQ	<i>Exp.</i>	Γ_i^{NR}	Γ_i^{NR+RC}	<i>Exp.</i>		Q	UQ	<i>Exp.</i>	Γ_i^{NR}	Γ_i^{NR+RC}	<i>Exp.</i>
1^1S_0	D^0	1865	1865	1865	–	–	–	D_s	1969	1969	1969	–	–	–
1^3S_1	D^*	2010	2010	2008	0.0647	0.0183	< 2.1	D_s^*	2112	2112	2112	–	–	–
				2010	0.1321	0.0375	0.0834							
2^1S_0	$D_0(2550)$	2554	2502	2518 ± 9	56	240	199 ± 22	$D_{s0}(2590)$	2655	2629	2591 ± 9	18	76	89 ± 20
2^3S_1	$D_1^*(2600)$	2640	2602	2627 ± 10	28	155	141 ± 23	$D_{s1}^*(2700)$	2738	2743	2714 ± 5	8	117	122 ± 10
1^3P_0	$D_0^*(2300)$	2307	2226	2297 ± 28	134	279	273 ± 60	$D_{s0}^*(2317)$	2400	2312	2318	–	–	< 3.8
$1P_1$	$D_1(2430)$	2422	2410	2412 ± 9	93	249	314 ± 29	$D_{s1}(2460)$	2522	2484	2460	–	–	< 3.5
$1P_1'$	$D_1(2420)$	2453	2435	2427.2 ± 2.2	21.5	12.5	23.2 ± 4.6	$D_{s1}(2536)$	2544	2518	2535	0.6	0.4	0.92 ± 0.05
1^3P_2	$D_2^*(2460)$	2475	2464	2461.1 ± 0.7	56.7	43.6	47.3 ± 0.8	$D_{s2}^*(2573)$	2574	2557	2569	21.3	17.9	16.9 ± 0.7
1^3D_1	–	2750	2645	–	103	105	–	$D_{s1}^*(2860)$	2838	2825	2859 ± 41	32	22	159 ± 122
$1D_2$	$D_2(2740)$	2757	2722	2751 ± 10	101	163	102 ± 32	–	2855	2869	–	28	26	–
$1D_2'$	–	2822	2789	–	67	54	–	–	2907	2890	–	27	25	–
1^3D_3	$D_3^*(2750)$	2782	2771	2753 ± 10	52	44	66 ± 24	$D_{s3}^*(2860)$	2879	2888	2860.5 ± 11.1	30	28	53 ± 17
		<i>B mesons</i>						<i>B_s mesons</i>						
$n^{2S+1}L_J$	Observed state	Mass (MeV)			Width (MeV)			Observed state	Mass (MeV)			Width (MeV)		
		Q	UQ	<i>Exp.</i>	Γ_i^{NR}	Γ_i^{NR+RC}	<i>Exp.</i>		Q	UQ	<i>Exp.</i>	Γ_i^{NR}	Γ_i^{NR+RC}	<i>Exp.</i>
1^1S_0	B^0	5280	5280	5280	–	–	–	B_s	5367	5367	5367	–	–	–
1^3S_1	B^*	5325	5325	5325	–	–	–	B_s^*	5416	5416	5416	–	–	–
2^1S_0	–	5877	5789	–	36	276	–	–	5964	5915	–	34	131	–
2^3S_1	$B_J(5840)^{+?}$	5902	5822	5851 ± 19	12	282	224 ± 104	–	5991	5953	–	27	181	–
1^3P_0	–	5695	5616	–	138	299	–	–	5775	5711	–	–	–	–
$1P_1$	–	5746	5691	–	127	311	–	–	5834	5781	–	–	–	–
$1P_1'$	$B_1(5721)^0$	5762	5730	5726.1 ± 1.3	29.0	16.5	27.5 ± 3.4	$B_{s1}(5830)$	5842	5810	5829	0.06	0.04	0.5 ± 0.4
1^3P_2	$B_2^*(5747)^0$	5769	5734	5739.5 ± 0.7	43.5	29.1	24.2 ± 1.7	$B_{s2}^*(5840)$	5857	5827	5840	2.79	2.07	1.49 ± 0.27
1^3D_1	–	6080	5951	–	131	152	–	–	6154	6149	–	62	40	–
$1D_2$	$B_J(5970)^0?$	6036	5955	5971 ± 5	89	105	81 ± 12	$B_{sJ}(6109)$	6123	6125	6108.8 ± 1.8	52	32	22 ± 9
$1D_2'$	–	6114	6049	–	88	83	–	$B_{sJ}(6158)$	6186	6159	6158 ± 9	43	42	72 ± 43
1^3D_3	–	6051	6004	–	56	47	–	–	6137	6116	–	35	35	–

TABLE IV: The mass shifts ΔM and partial widths (in MeV) of the D and D_s states. The bare masses obtained from the potential model are listed in square brackets. The strong decay widths, which combine the unquenched spectra and are described by non-relativistic chiral interactions \mathcal{H}_i^{NR} , are further augmented by a relativistic correction term \mathcal{H}_i^{RC} . These widths are denoted as Γ_i^{NR} and Γ_i^{NR+RC} , respectively. The forbidden decay channel is denoted by "...". The experimental data are taken from the PDG [6].

$D(2^1S_0)$				$D(2^3S_1)$			$D(1^3P_0)$				$D(1^3P_2)$				
Channel	ΔM	$as D_0(2550)$		ΔM	$as D_1^*(2600)$		Channel	ΔM	$as D_0^*(2300)$		Channel	ΔM	$as D_2^*(2460)$		
	[2575]	Γ_i^{NR}	Γ_i^{NR+RC}		[2667]	Γ_i^{NR}		Γ_i^{NR+RC}	[2304]	Γ_i^{NR}		Γ_i^{NR+RC}	[2510]	Γ_i^{NR}	Γ_i^{NR+RC}
$D\pi$	4.4	11.2	31.0	$D\pi$	-78.1	134.0	279.4	$D\pi$	-19.3	35.7	29.0	
$D^*\pi$	-36.2	43.1	225.6	-2.1	0.4	92.0	$D^*\pi$	$D^*\pi$	-24.5	20.9	14.5	
$D\eta$	-0.6	0.02	4.2	$D\eta$	$D\eta$	-2.1	0.1	0.1	
$D^*\eta$	-2.2	0.7	3.9	$Total$	-78.1	134.0	279.4	$Total$	-45.9	56.7	43.6	
$D_s K$	-1.4	1.8	4.1	$Exp.$	-	273 ± 60	-	$Exp.$	-	47.3 ± 0.8	-	
$D_s^* K$	-2.8	0.03	1.0	$D(1P_1)$				$D(1P_1')$				
$D_0^*(2300)\pi$	-36.3	13.0	14.3	Channel	ΔM	$as D_1(2430)$		Channel	ΔM	$as D_1(2420)$		
$D_1(2430)\pi$	-43.6	14.0	18.9	[2449]	[2449]	Γ_i^{NR}	Γ_i^{NR+RC}	[2471]	[2471]	Γ_i^{NR}	Γ_i^{NR+RC}	
$D_1(2420)\pi$	-6.7	0.2	0.02	$D^*\pi$	-39.3	92.9	249.2	$D^*\pi$	-36.1	21.5	12.5	
$D_2^*(2460)\pi$	-10.4	0.02	0.01	$Total$	-39.3	92.9	249.2	$Total$	-36.1	21.5	12.5	
$Total$	-72.5	56.1	239.9	-65.4	28.4	155.1	$Exp.$	-	314 ± 29	-	$Exp.$	-	23.2 ± 4.6	-	
$Exp.$	-	199 ± 22	-	-	141 ± 23	-	$D(1D_2)$				$D(1D_2')$				
$D(1^3D_1)$				$D(1^3D_3)$			$D(1D_2)$				$D(1D_2')$				
Channel	ΔM	$M = 2645$		Channel	ΔM	$as D_3^*(2750)$		Channel	ΔM	$as D_2(2740)$		Channel	ΔM	$M = 2789$	
[2765]	[2765]	Γ_i^{NR}	Γ_i^{NR+RC}	[2830]	[2830]	Γ_i^{NR}	Γ_i^{NR+RC}	[2799]	[2799]	Γ_i^{NR}	Γ_i^{NR+RC}	[2856]	[2856]	Γ_i^{NR}	Γ_i^{NR+RC}
$D\pi$	-2.9	18.7	10.1	$D\pi$	-7.6	20.0	21.2	$D^*\pi$	-3.9	17.3	23.1	$D^*\pi$	-20.1	36.8	31.7
$D^*\pi$	-1.8	7.8	4.5	$D^*\pi$	-11.5	18.4	17.4	$D^*\eta$	-0.8	4.7	2.1	$D^*\eta$	-2.5	1.3	1.0
$D\eta$	-0.5	4.2	0.9	$D\eta$	-1.1	1.2	1.3	$D_s^* K$	-1.9	8.6	2.3	$D_s^* K$	-4.9	1.3	0.8
$D^*\eta$	-0.3	0.8	0.2	$D^*\eta$	-1.4	0.5	0.4	$D_0^*(2300)\pi$	-1.8	5E-3	0.5	$D_0^*(2300)\pi$	-13.5	10.7	11.9
$D_s K$	-1.3	8.8	0.3	$D_s K$	-1.6	0.9	0.9	$D_1(2430)\pi$	-4.2	0.4	0.5	$D_1(2430)\pi$	-0.3	2.9	3E-3
$D_s^* K$	-0.6	0.6	0.03	$D_s^* K$	-2.7	0.3	0.3	$D_1(2420)\pi$	-5.2	0.7	0.5	$D_1(2420)\pi$	-10.6	9.0	0.8
$D_1(2430)\pi$	-9.0	0.02	0.2	$D_1(2430)\pi$	-4.2	5.6	0.8	$D_2^*(2460)\pi$	-56.5	66.3	130.3	$D_2^*(2460)\pi$	-14.6	3.8	6.3
$D_1(2420)\pi$	-90.1	62.0	88.9	$D_1(2420)\pi$	-11.0	1.1	0.4	$D\rho$	-2.1	2.5	2.5	$D\rho$	-0.5	1.0	1.0
$D_2^*(2460)\pi$	-12.8	0.02	0.01	$D_2^*(2460)\pi$	-17.2	3.7	1.1	$D\omega$	-0.7	0.7	0.7	$D\omega$	-0.2	0.3	0.3
$D\rho$	-0.2	1E-5	1E-5	$D\rho$	-0.4	0.1	0.1	$Total$	-77.1	101.2	162.6	$Total$	-67.2	67.1	53.8
$D\omega$	-0.06	$D\omega$	-0.1	0.03	0.03	$Exp.$	-	102 ± 32	-	$Exp.$	-	-	-
$Total$	-119.6	102.9	105.1	$Total$	-58.8	51.8	43.9	$D_s(1^3P_0)$				$D_s(1^3P_2)$			
$Exp.$	-	-	-	$Exp.$	-	66 ± 5	-	Channel	ΔM	$as D_{s0}^*(2317)$		Channel	ΔM	$as D_{s2}^*(2573)$	
$D_s(2^1S_0)$				$D_s(2^3S_1)$			$D_s(1^3P_0)$				$D_s(1^3P_2)$				
Channel	ΔM	$as D_{s0}(2590)$		Channel	ΔM	$as D_{s1}^*(2700)$		[2372]	[2372]	Γ_i^{NR}	Γ_i^{NR+RC}	[2597]	[2597]	Γ_i^{NR}	Γ_i^{NR+RC}
[2677]	[2677]	Γ_i^{NR}	Γ_i^{NR+RC}	[2753]	[2753]	Γ_i^{NR}	Γ_i^{NR+RC}	DK	-60.0	DK	-17.9	19.0	16.1
DK	DK	2.1	3.7	31.0	$D^* K$	$D^* K$	-20.1	2.2	1.7
$D^* K$	-47.7	17.9	76.2	$D^* K$	-8.0	3.7	76.8	$D_s \eta$	$D_s \eta$	-2.0	0.1	0.1
$D_s \eta$	$D_s \eta$	-0.7	0.6	5.8	$Total$	-60.0	-	-	$Total$	-40.0	21.3	17.9
$D_s^* \eta$	$D_s^* \eta$	-3.6	0.1	3.4	$Exp.$	-	< 3.8	-	$Exp.$	-	16.9 ± 0.7	-
$Total$	-47.7	17.9	76.2	$Total$	-10.2	8.1	117.0	$D_s(1P_1)$				$D_s(1P_1')$			
$Exp.$	-	89 ± 20	-	$Exp.$	-	122 ± 10	-	Channel	ΔM	$as D_{s1}(2460)$		Channel	ΔM	$as D_{s1}(2536)$	
$D_s(1^3D_1)$				$D_s(1^3D_3)$			$D_s(1P_1)$				$D_s(1P_1')$				
Channel	ΔM	$as D_{s1}^*(2860)$		Channel	ΔM	$as D_{s3}^*(2860)$		[2533]	[2533]	Γ_i^{NR}	Γ_i^{NR+RC}	[2546]	[2546]	Γ_i^{NR}	Γ_i^{NR+RC}
[2829]	[2829]	Γ_i^{NR}	Γ_i^{NR+RC}	[2909]	[2909]	Γ_i^{NR}	Γ_i^{NR+RC}	$D^* K$	-49.3	$D^* K$	-28.1	0.6	0.4
DK	-1.5	14.9	13.1	DK	-7.3	16.7	16.0	$Total$	-49.3	-	-	$Total$	-28.1	0.6	0.4
$D^* K$	-1.0	7.8	7.0	$D^* K$	-10.8	12.0	10.7	$Exp.$	-	< 3.5	-	$Exp.$	-	0.92 ± 0.05	-
$D_s \eta$	-1.2	7.3	1.6	$D_s \eta$	-0.8	0.9	0.6	$D_s(1D_2)$				$D_s(1D_2')$			
$D_s^* \eta$	-0.6	2.4	0.6	$D_s^* \eta$	-1.5	0.4	0.3	Channel	ΔM	$M = 2869$		Channel	ΔM	$M = 2890$	
DK^*	-0.1	0.04	0.03	DK^*	-0.4	0.1	0.1	[2877]	[2877]	Γ_i^{NR}	Γ_i^{NR+RC}	[2923]	[2923]	Γ_i^{NR}	Γ_i^{NR+RC}
$Total$	-4.4	32.4	22.3	$Total$	-20.8	30.1	27.7	$D^* K$	-2.4	18.7	20.8	$D^* K$	-18.2	24.4	22.1
$Exp.$	-	159 ± 122	-	$Exp.$	-	53 ± 17	-	$D_s^* \eta$	-1.5	6.4	2.8	$D_s^* \eta$	-2.5	1.2	0.8
$D_s(1^3D_1)$				$D_s(1^3D_3)$			$D_s(1D_2)$				$D_s(1D_2')$				
Channel	ΔM	$as D_{s1}^*(2860)$		Channel	ΔM	$as D_{s3}^*(2860)$		Channel	ΔM	$M = 2869$		Channel	ΔM	$M = 2890$	
[2829]	[2829]	Γ_i^{NR}	Γ_i^{NR+RC}	[2909]	[2909]	Γ_i^{NR}	Γ_i^{NR+RC}	[2877]	[2877]	Γ_i^{NR}	Γ_i^{NR+RC}	[2923]	[2923]	Γ_i^{NR}	Γ_i^{NR+RC}
DK	-1.5	14.9	13.1	DK	-7.3	16.7	16.0	$D_0^*(2300)K$	-1.5	2E-6	4E-4	$D_0^*(2300)K$	-11.5	0.8	0.9
$D^* K$	-1.0	7.8	7.0	$D^* K$	-10.8	12.0	10.7	DK^*	-2.3	2.9	2.8	DK^*	-0.5	0.9	1.0
$D_s \eta$	-1.2	7.3	1.6	$D_s \eta$	-0.8	0.9	0.6	$Total$	-7.7	28.0	26.4	$Total$	-32.7	27.3	24.8
$D_s^* \eta$	-0.6	2.4	0.6	$D_s^* \eta$	-1.5	0.4	0.3	$Exp.$	-	-	-	$Exp.$	-	-	-
DK^*	-0.1	0.04	0.03	DK^*	-0.4	0.1	0.1	$D_s(1D_2)$				$D_s(1D_2')$			
$Total$	-4.4	32.4	22.3	$Total$	-20.8	30.1	27.7	Channel	ΔM	$M = 2869$		Channel	ΔM	$M = 2890$	
$Exp.$	-	159 ± 122	-	$Exp.$	-	53 ± 17	-	[2877]	[2877]	Γ_i^{NR}	Γ_i^{NR+RC}	[2923]	[2923]	Γ_i^{NR}	Γ_i^{NR+RC}

TABLE V: The mass shifts ΔM and partial widths (in MeV) of the B and B_s states. The bare masses obtained from the potential model are listed in square brackets. The strong decay widths, which combine the unquenched spectra and are described by non-relativistic chiral interactions \mathcal{H}_i^{NR} , are further augmented by a relativistic correction term \mathcal{H}_i^{RC} . These widths are denoted as Γ_i^{NR} and Γ_i^{NR+RC} , respectively. The forbidden decay channel is denoted by "...". The experimental data are taken from the PDG [6].

$B(2^1S_0)$				$B(2^3S_1)$			$B(1^3P_0)$			$B(1^3P_2)$		
Channel	ΔM	$M = 5789$		ΔM	$as B_J(5840)^+$		ΔM	$M = 5616$		ΔM	$as B_2^*(5747)^{+/0}$	
	[5882]	Γ_i^{NR}	Γ_i^{NR+RC}		[5908]	Γ_i^{NR}		Γ_i^{NR+RC}	[5704]		Γ_i^{NR}	Γ_i^{NR+RC}
$B\pi$	-2.5	0.2	95.9				-19.5	21.9/22.4	15.1/15.5
$B^*\pi$	-34.8	18.8	256.7	-13.2	3.7	175.5				-26.0	20.5/21.1	13.1/13.6
$B\eta$	-1.4	0.2	1.0						
$B^*\eta$	-2.1						
$B_s K$	-2.1						
$B_s^* K$	-3.5						
$B(1^3P_0)\pi$	-58.2	17.1	18.9						
$B(1P_1)\pi$	-44.9	7.9	9.2						
$B_1(5721)\pi$	-6.1						
$B_2^*(5747)\pi$	-10.0						
Total	-93.0	35.9	275.6	-85.8	12.0	281.6				-45.5	42.4/43.5	28.2/29.1
Exp.	-	-	-	-	224 ± 104	-				-	24.2 ± 1.7/20 ± 5	-
$B(1^3D_1)$				$B(1^3D_3)$			$B(1P_1)$			$B(1P_1')$		
Channel	ΔM	$M = 5951$		ΔM	$M = 6004$		ΔM	$M = 5691$		ΔM	$as B_1(5721)^{+/0}$	
	[6095]	Γ_i^{NR}	Γ_i^{NR+RC}		[6070]	Γ_i^{NR}		Γ_i^{NR+RC}	[5757]		Γ_i^{NR}	Γ_i^{NR+RC}
$B\pi$	-4.6	24.1	18.2	-11.8	22.7	22.8				-41.3	29.0/29.0	16.5/16.5
$B^*\pi$	-2.4	11.7	7.9	-15.3	23.9	22.8				-66.2	126.5	310.7
$B\eta$	-0.7	4.4	0.9	-1.4	0.5	0.5				-41.3	29.0/29.0	16.5/16.5
$B^*\eta$	-0.3	1.3	0.2	-1.6	0.3	0.2				-66.2	126.5	310.7
$B_s K$	-1.6	7.0	0.1	-2.0	0.2	0.2				-41.3	29.0/29.0	16.5/16.5
$B_s^* K$	-0.8	1.1	0.02	-3.3	0.1	0.1				-41.3	29.0/29.0	16.5/16.5
$B(1P_1)\pi$	-11.2	0.1	1.7	-2.1	5.5	0.2				-41.3	29.0/29.0	16.5/16.5
$B_1(5721)\pi$	-105.8	81.3	123.2	-12.9	0.5	0.1				-41.3	29.0/29.0	16.5/16.5
$B_2^*(5747)\pi$	-16.7	0.1	0.1	-15.4	1.9	0.4				-41.3	29.0/29.0	16.5/16.5
Total	-144.1	131.1	152.2	-65.8	55.6	47.3				-41.3	29.0/29.0	16.5/16.5
Exp.	-	-	-	-	-	-				-	27.5 ± 3.4/31 ± 6	-
$B_s(2^1S_0)$				$B_s(2^3S_1)$			$B(1D_2)$			$B(1D_2')$		
Channel	ΔM	$M = 5915$		ΔM	$M = 5953$		ΔM	$M = 5955$		ΔM	$M = 6049$	
	[5969]	Γ_i^{NR}	Γ_i^{NR+RC}		[5996]	Γ_i^{NR}		Γ_i^{NR+RC}	[6055]		Γ_i^{NR}	Γ_i^{NR+RC}
BK	-9.4	7.4	70.1				-28.5	55.4	52.8
B^*K	-53.6	34.3	131.1	-25.8	19.3	108.0				-3.3	1.4	1.1
$B_s\eta$	-3.4	0.05	2.6				-6.1	1.3	0.7
$B_s^*\eta$	-4.7				-14.7	14.7	18.8
Total	-53.6	34.3	131.1	-43.3	26.8	180.7				-0.6	3.7	0.4
Exp.	-	-	-	-	-	-				-9.1	6.5	0.1
$B_s(1^3D_1)$				$B_s(1^3D_3)$			$B_s(1P_1)$			$B_s(1P_1')$		
Channel	ΔM	$M = 6149$		ΔM	$M = 6116$		ΔM	$M = 5781$		ΔM	$as B_{s1}(5830)^0$	
	[6156]	Γ_i^{NR}	Γ_i^{NR+RC}		[6146]	Γ_i^{NR}		Γ_i^{NR+RC}	[5840]		Γ_i^{NR}	Γ_i^{NR+RC}
BK	-2.7	28.3	24.3	-11.8	17.6	17.9				-31.5	0.06	0.04
B^*K	-1.7	15.2	11.7	-15.0	16.4	16.0				-59.3	0.06	0.04
$B_s\eta$	-1.6	12.9	2.5	-1.2	0.4	0.4				-	0.06	0.04
$B_s^*\eta$	-0.8	5.3	1.0	-2.0	0.4	0.3				-	-	0.5 ± 0.4
Total	-6.8	61.7	39.5	-30.0	34.8	34.6				-	-	-
Exp.	-	-	-	-	-	-				-	-	-
$B_s(1^3D_2)$				$B_s(1^3D_2')$			$B_s(1D_2)$			$B_s(1D_2')$		
Channel	ΔM	$M = 6109$		ΔM	$M = 6158$		ΔM	$M = 5711$		ΔM	$as B_{s2}^*(5840)^0$	
	[6131]	Γ_i^{NR}	Γ_i^{NR+RC}		[6191]	Γ_i^{NR}		Γ_i^{NR+RC}	[5772]		Γ_i^{NR}	Γ_i^{NR+RC}
B^*K	-4.2	41.4	29.9	-28.2	41.7	40.5				-16.1	2.56	1.91
$B_s^*\eta$	-2.2	10.5	2.2	-3.6	1.7	1.2				-20.7	0.23	0.16
Total	-6.4	51.9	32.1	-31.8	43.4	41.7				-60.9	-	2.07
Exp.	-	22 ± 9	-	-	-	-				-	-	1.49 ± 0.27